

# A Study on Access Impedance for Vehicular Power Line Communications

Nima Taherinejad, Roberto Rosales, Shahriar Mirabbasi and Lutz Lampe

ECE Dep., University of British Columbia, Vancouver, Canada

{nimat, robertor, shahriar, lampe}@ece.ubc.ca

**Abstract**—In this paper, we present an experimental study of access impedance for vehicular power line communications (VPLC). This study aims to provide better understanding of the effects of the vehicle loads on the impedance of the VPLC plug-in access nodes. Also, some insights for the design of adaptive impedance matching are provided. We report impedance measurements of various loads and car battery, which combined with input impedance measurements from a specific sport car are used to calculate an equivalent access impedance of a PLC device connected in parallel. We show how the inductive nature of the loads dominates the overall access impedance making it on one hand more attractive for transmission in the high MHz range, and on the other more challenging for the implementation of impedance matching.

**Keywords**- *Vehicular Power Line Communication; Adaptive Impedance Matching, Access Impedance; Load Impedance Measurement.*

## I. INTRODUCTION

Power line communications (PLC) reuses existing power lines for communication purposes, which renders itself as a frugal solution to establish communication links in many situations. While the beginnings of PLC technology go back to the early 1900s, where it has been used by electricity utilities for voice communications and automation and control [1], it has only reached broader public attention with the introduction of broadband over power lines since the 1990s [2], [3]. More recently, the use of power lines to establish data communications in vehicles has become another application of PLC, cf. e.g., [4]-[13]. The reason for this is the significant growth of the number of electronic components and systems in vehicles, which leads to an increased demand for data traffic and number of data communication points. To enable this data traffic, a considerable amount of extra wires dedicated for communication purposes is usually installed. These extra wires contribute notably to cost, weight, volume, and complexity of vehicles [14], [15]. Therefore, vehicular PLC (VPLC), which makes additional wires dedicated for data communication unnecessary, provides the distinct advantage of a simplified, lighter, and less expensive wiring harness [7], [16].

To design suitable data transmission equipments, a good understanding of the communication channel characteristics is essential. For example, an important issue of VPLC is to maintain reliable communication over highly frequency selective channels [11]. Frequency selectivity is caused by impedance mismatches in the wiring harness, which clearly had not been designed with data communication in mind [8]. Another important and rather unique characteristic of PLC is

This work is supported in part by the AUTO21 Network of Centres of Excellence, the National Sciences and Engineering Research Council of Canada (NSERC), the Institute for Computing, Information and Cognitive Systems (ICICS) at UBC, and Partners for the Advancement of Collaborative Engineering Education (PACE) program.

that the network access impedance varies with location (point of access to the power line network), frequency, and time. This characteristic renders impedance matching an appealing concept [2]. However, matching the network access impedance with preferably simple passive circuits is challenging due to the mentioned frequency selectivity. To study the design of adaptive coupling units and possible gains achievable for VPLC, it is important to know typical ranges of access impedances in vehicles.

In this paper, we continue the investigations by our group, started in [13], and by others, e.g., [6], [9], [11], [12], towards a better understanding and modeling of the VPLC channel. In particular, although battery and loads have been identified as important network elements [11], whose characteristics have a notable impact on channel transfer function and access impedances, there is little measurement data on these components available in the open literature. Intending to close this gap, we present measurement results for battery load impedances and discuss their impact on the network access impedances. TABLE 1 illustrates the frequency bands considered in a number of previous studies and commercial solutions for VPLC. To provide results relevant and applicable to the wide range of frequency bands envisaged for VPLC, for this study we performed all our measurements up to 100MHz.

TABLE 1 REPORTED VPLC FREQUENCY BANDS

Commercial solutions	[17] carriers: (1.75, 4.5, 5.5, 6, 6.5, 10.5, 13)MHz [18] carriers: (4.49-20.7)MHz
Test beds	[19] (0-30MHz) Homeplug v1.0, Spidcom [20] (2-28)MHz HPAV, HD-PLC
Channel studies	[6] (0-30)MHz [20] (3-50)MHz [9] (0.5-70)MHz [13] (.1-100)MHz [8]
Frequency band (MHz)	10 20 30 40 50 70 100 >100

The remainder of this paper is organized as follows. In Section II, stand-alone battery and load measurements are presented and discussed. In Section III, access impedance is broadly studied. This includes input impedance measurements at several access points and discussions on the impact of the load impedances on the overall access impedance. Finally, Section IV concludes the paper.

## II. BATTERY AND LOAD MEASUREMENTS

In this section we describe impedance measurements of five loads and one car battery from a Pontiac Solstice 2006 sport vehicle. Considering various potential applications of VPLC technology, we selected the following plug-in locations: front and rear lamp for sensors, and battery, cigarette lighter, and trunk light for main control units. These load choices are made based on the fact that their locations are reasonable access points for potential PLC-based applications such as car rear/back-up camera, front and rear radar collision systems, or a control system that is being charged through the cigarette lighter.

### A. Measurement Setup

For all measurements the device under test is disconnected from the vehicle and tested stand-alone using an Agilent 8793E vector network analyzer (VNA). The corresponding complex input impedances are afterwards calculated from the measured S11 data. The measurement frequency range is set from 100kHz to 100MHz. In order to connect the different load terminals to the VNA coaxial test ports, we used custom made adaptors. These adaptors were designed and realized in a way that VNA Port Extension could be used to compensate for their electrical length.

### B. Battery

The typical distance between the battery's (+) and (-) terminals represents an obstacle for VNA measurements in the MHz range, as it forces splitting the VNA coaxial signal and coaxial ground several inches apart to be able to make electrical contact with the battery terminals. Such splitting is a significant cause of errors as it creates an equivalent 'ground lead' connection to the battery's (-) terminal. To solve this problem, we built a microstrip line on a printed-circuit board (PCB) that, when inserted on top of the battery, provides a suitable RF connection between the battery terminals and a coaxial cable. The PCB, shown in Fig. 1, allows us to obtain repetitive and resonance-free impedance measurements.

Results from the battery S11 measurements show that the battery's internal impedance consists of a series resistive and inductive part, shown in Figs. 2 and 3.



Figure 1. Microstrip interface PCB for 1-Port VNA measurements of the car battery.

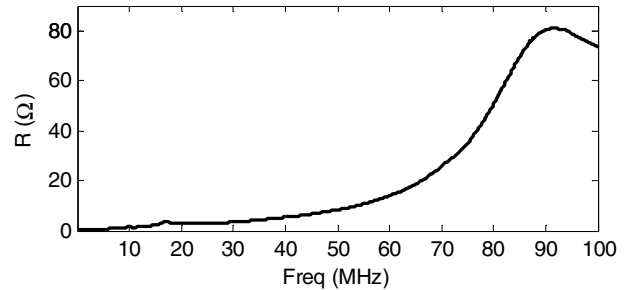


Fig. 2. Resistive part of battery internal impedance.

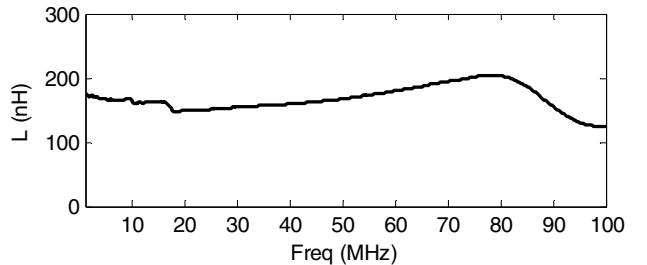


Fig. 3. Inductive part of battery internal impedance.

As seen on Fig. 2, the output resistance of the battery at low frequencies is almost zero and gradually increases reaching  $10\Omega$  at 50MHz. Therefore, as expected, at the lowest frequencies, the battery acts as an ideal voltage source with negligible output resistance. For a VPLC modem connected near the battery this would represent having a short circuit connected in parallel. Beyond 50MHz the impedance rapidly increases until reaching a peak of  $80\Omega$ , thus improving the prospects for a nearby PLC modem.

From Fig. 3, the battery's output inductance is close to a constant value of approximately  $150\text{nH}$ . This means that the output reactance of the battery will increase linearly with frequency. Thus both real and imaginary parts of the battery's impedance increase with frequency.

Given the inner configuration of the battery cells, an inductive behavior may seem counterintuitive and possibly the result of a measurement artifact. Nonetheless, the high-frequency inductive nature of batteries is a phenomenon that has been observed and studied for sealed lead-acid batteries in [21]. In addition, we must emphasize that the microstrip adapter shown in Fig. 1 is the result of our efforts to eliminate unwanted measurement errors, mostly caused by magnetic coupling. In that sense, the circuit successfully allowed us to obtain a calibrated measurement plane, and repeatable measurements, regardless of the position of the VNA cable.

### C. Load Measurements

To measure the lamps stand-alone, we use simple custom adaptors carefully crafted such that their electrical length could be easily de-embedded by the VNA. Measurements are taken at the ON and OFF states. Given the large currents required to turn the lamps on (up to  $5\text{A}$ ), we could not use the built-in Bias Tee of the VNA, for which the maximum current limit is  $500\text{mA}$ . Instead we connected a battery in parallel, and carefully de-embedded its effect from the measurements. Results show again a series resistive and inductive part. The

resistive behavior is as expected low in the OFF state, and higher at the ON state, with ON values that correspond to the lamps quoted wattage. The measurement results are summarized in TABLE 2.

On the other hand the inductive behavior is found to be the same for the ON and OFF states, and not linear with frequency. To simplify future modeling of the inductances, a least squares third-order polynomial fitting of the data is performed. The resulting coefficients are listed in TABLE 2, and can be used to calculate the inductance  $L$  as follows:

$$L = L_o + L_1 \cdot f + L_2 \cdot f^2 + L_3 \cdot f^3 \quad (1)$$

As examples, Fig. 4 shows the measured inductances and the fitted curves for the rear tail, trunk, and the front low and high beam lamps.

TABLE 2 MEASUREMENT RESULTS FOR LOAD IMPEDANCES

Loads (Lamps)	Resistance $\Omega$		$L_0$ $H$	$L_1$ $H/Hz$	$L_2$ $H/Hz^2$	$L_3$ $H/Hz^3$
	Off	On	$10^{-9}$	$10^{-18}$	$10^{-25}$	$10^{-34}$
Front High Beam	0.24	2.36	130.1	-404.5	90.3	-242.9
Front Low Beam	0.37	2.74	177.6	-751.1	161.9	-308.7
Rear – Tail	6.59	25.2	309.0	-7701	1384	-7344
Trunk	2.43	12.8	112.5	-122.6	25.1	-7.1

### III. ACCESS IMPEDANCE

We now move on to consider the access impedance  $Z_{IN}$  experienced at different locations of a VPLC network. Knowledge of typical ranges of  $Z_{IN}$  is essential for the emulation of VPLC networks and the design of adaptive impedance matching circuits.

#### A. Obtaining the Network Impedance

We consider as access impedance,  $Z_{ACCESS}$ , the impedance seen at the transmitting terminals of a PLC device (transmitter/receiver) when connected in parallel to a PLC plug-in point. Our approach to determine  $Z_{ACCESS}$  for the selected potential plug-in points consists of measuring with a VNA the network input impedance  $Z_{NWK}$  at each of the selected plug-in nodes, after which we calculate each  $Z_{ACCESS}$  from the parallel combination of the loads measured in Section II with their corresponding measured  $Z_{NWK}$ .

During the measurement of each  $Z_{NWK}$  we have proceeded as follows:

- For each of the Lamps, we have removed the lamp from the vehicle and measured the network impedance  $Z_{NWK}$ , at the lamp's plug-in node, with all other loads of the network attached. For the Rear and Front lamps we have taken measurements with the lamp switch turned ON and OFF.
- For the Cigarette Lighter, we have measured the network impedance  $Z_{NWK}$  directly with all other loads attached to the network. Notice that since there are no loads connected to this point  $Z_{ACCESS} = Z_{NWK}$ .

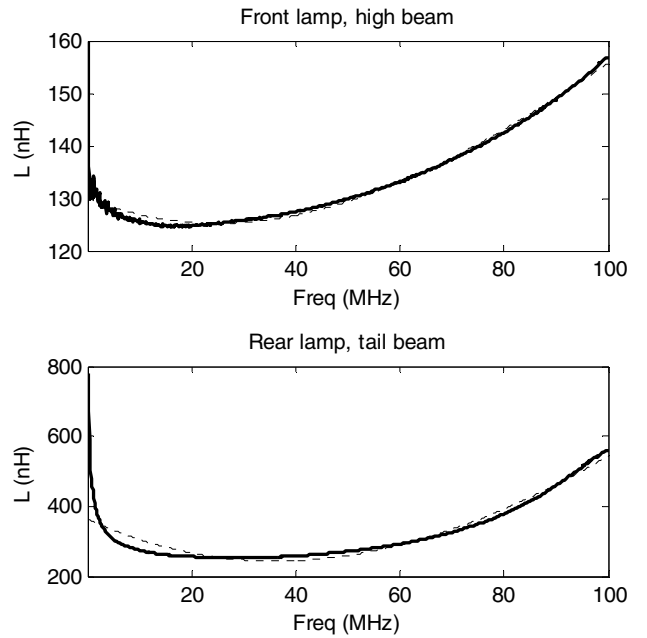


Fig. 4. Lamp inductances: (top) Front Lamp high beam, (bottom) Rear Tail Lamp. Measured (solid) and Fitted Curve (dashed)

- For the Battery we have measured the network impedance at the battery terminals with the battery still attached. This is possible by placing the interface board described in Section II between the battery and the battery terminals.

#### B. Measured Network Impedances

In Figs. 5, 6 and 7, we show the measured input impedances  $Z_{NWK}$ , obtained from the car network. For all plots scattering parameters (S parameters) measured with the VNA are used to calculate the corresponding input impedances. All connector adaptors are carefully de-embedded from the measurements. Notice the sudden spikes in the resistance and the sudden capacitive to inductive changes in the reactance, which interestingly are more pronounced at the lower frequencies, and which present a challenge for the design of adaptive impedance matching circuits.

Fig. 5 shows the real and imaginary parts of  $Z_{NWK}$  for the rear, front and trunk lamps while turned ON. This means that even though the lamps have been removed from the network their ON/OFF relays in the car are switched ON. Fig. 6 shows the measurement results for the Front and Rear lamps when turned OFF. It can be seen that the reactance of most lamps is initially capacitive. We attribute this behavior to the open contact capacitance of the lamp relays, which we have measured with the VNA to be in the range of 1.6pF to 1.83pF. Surprisingly, however, there are two reactances, corresponding to the rear tail lamps, which are initially inductive at low frequencies.

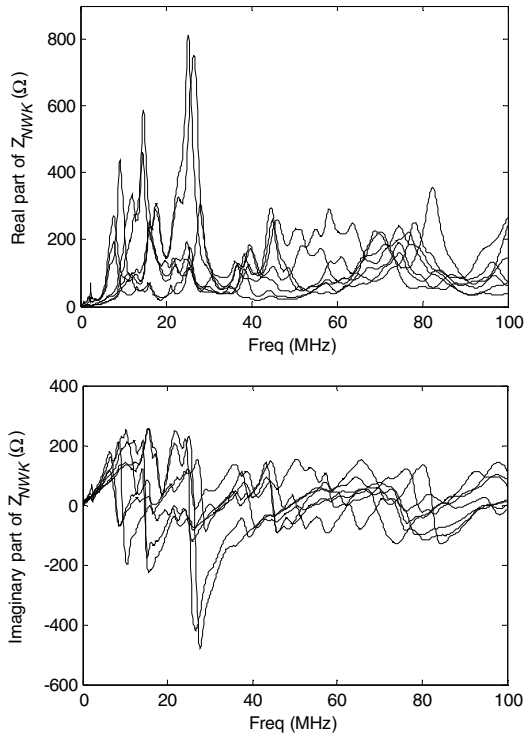


Fig.5. Measured Network Input Impedances  $Z_{\text{NWK}}$  at Rear, Front, and Trunk lamp access nodes while turned ON  
(top) Real Part, (bottom) Imaginary Part.

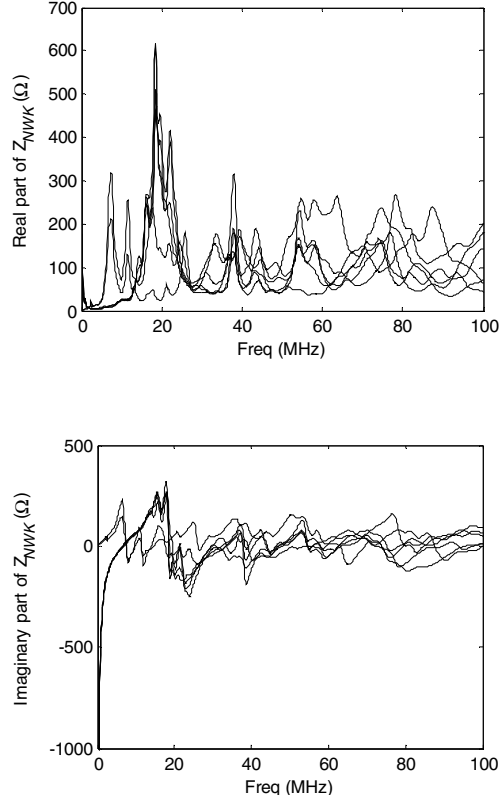


Fig.6. Measured Network Input Impedances  $Z_{\text{NWK}}$  at Rear and Front lamp access nodes while turned OFF  
(top) Real Part, (bottom) Imaginary Part

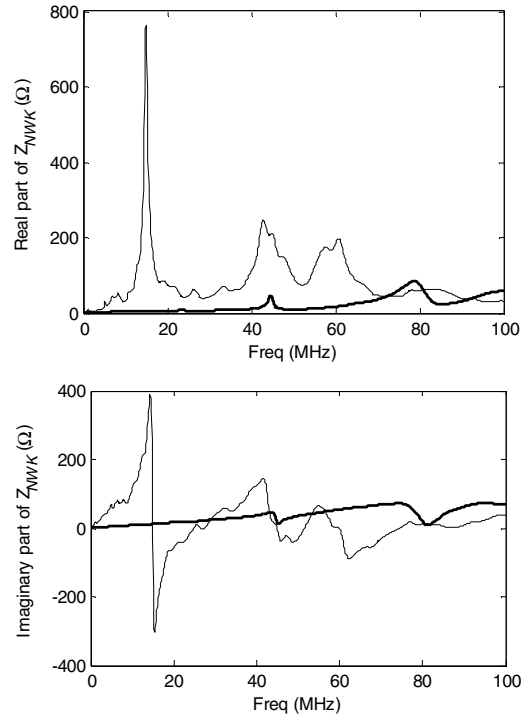


Fig.7. Measured Network Input Impedances  $Z_{\text{NWK}}$  at Cigarette Lighter (thin line) and Battery (bold line)  
(top) Real Part, (bottom) Imaginary Part.

Fig. 7 corresponds to the cigarette lighter (thin lines) and the battery (bold lines) plug-in points. Because the cigarette lighter is located near the battery with only one fuse in between we were expecting the  $Z_{\text{NWK}}$  at the cigarette lighter to be the closest to the impedance measured at the battery. However, results show otherwise. Nonetheless we can still not rule out the possibility of resonance caused by our custom SMA coax to cigar lighter connector adapter. On the other hand, at the battery node the impedance is dominated by the inductive nature of the battery.

### C. Total Access Impedances

At first glance, the results shown in the previous subsection seem to indicate that the lower frequency range is the most adverse frequency band for implementation of an (adaptive) impedance matching circuit. However, we still need to take into account the effect of the vehicle loads when connected in parallel to the plug-in access nodes. As explained earlier we obtain the total Access Impedances,  $Z_{\text{ACCESS}}$ , by calculating the impedance that results from the parallel connection of the load data measured in Section II-A, with the network input impedance measured in Section III-B.

Fig. 8 shows the resulting values of  $Z_{\text{ACCESS}}$  for all lamps in the ON state. As we can observe from the figure the total access impedance is strongly influenced by the inductive nature of the loads. Similarly to the case of the battery, a modem connected to any of the lamp plug-in nodes will experience a practical short-circuit near DC, and an increasing output load with frequency. This effect is also present when the lamps are at their OFF state, as shown in Fig. 9. The real part of  $Z_{\text{ACCESS}}$

for the OFF state is not shown since it is approximately the same as that of Fig. 8. For the Cigarette Lighter and the Battery plug-in nodes  $Z_{\text{ACCESS}}$  is the same as shown on Fig. 7, since there are no other loads at those nodes to consider in parallel.

#### D. Discussion

Based on our measurements, the battery appears as an inductive load; at low frequencies this supports the concept of direct and indirect paths as suggested in [9], where a ‘direct’ PLC data connection that does not pass through the battery is more desirable to avoid being short-circuited to ground by the battery’s low impedance.

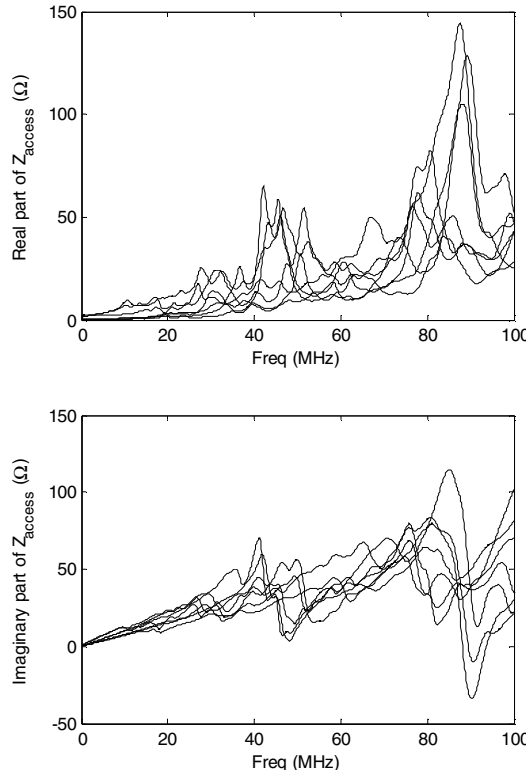


Fig. 8. Calculated Access Input Impedances  $Z_{\text{ACCESS}}$ . at Rear, Front, and Trunk lamp access nodes while turned ON  
(top) Real Part, (bottom) Imaginary Part.

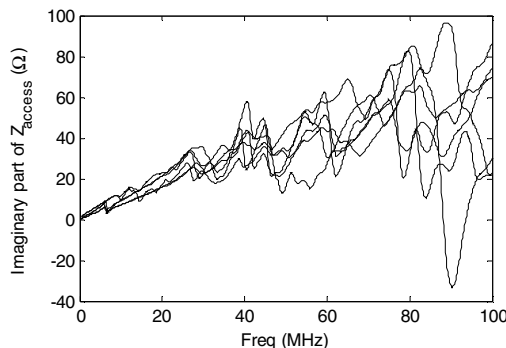


Fig. 9. Imaginary Part of Calculated Access Input Reactance  $Z_{\text{ACCESS}}$ . at Rear and Front lamp access nodes while turned OFF.

On the other hand at higher frequencies the battery’s impedance is significantly higher (both in resistance and reactance), acting more like an open circuit that allows the flow of data.

Furthermore, based on our load measurements, the lamps also behave like an inductive load over a wide frequency range (from ~DC to 100MHz) and their inductance is independent of whether the lamp is turned on or off. Their resistance changes slightly between the ON and OFF states. The existence of relays in a path does not necessarily mean that the path is completely open when the relay is off. It appears that the parasitic capacitance of the relays (when they are off) provides a capacitive path that conducts particularly at higher frequencies. We measured the parasitic capacitance of typical relays and their value ranges from 1.6pF to 1.83pF.

The inductive loads play a dominant role on the behavior of the access impedance, making impedance driving and/or matching more difficult for low frequencies, and easier for higher frequencies. This effect is so strong that it even dominates when  $Z_{\text{NWK}}$  is capacitive such as when the lamps are in their OFF state, (for example refer to the bottom diagram in Fig. 6). However, one could argue that even though, at lower frequencies, the inductive loads reduce the  $Z_{\text{ACCESS}}$ , they also reduce the variations of  $Z_{\text{NWK}}$ , making it a more controllable environment for impedance matching. While the scenario is totally reversed at higher frequencies, where both resistance and reactance vary significantly (e.g., Fig. 8).

An alternative approach to bypass the smaller  $Z_{\text{ACCESS}}$  at low frequencies would be to take advantage of the almost short-circuited path provided by the loads and connect the PLC modem in series with the load (since the load provides a low-impedance path to ground).

Comparing the obtained reactance limits of  $Z_{\text{ACCESS}}$  with those of  $Z_{\text{NWK}}$ , the reactance of  $Z_{\text{ACCESS}}$  is less in magnitude at higher frequencies, i.e., the parallel of  $Z_{\text{NWK}}$  with  $Z_{\text{load}}$  results in more reasonable reactances, from the point of view of the designer of an impedance matching circuit. In particular, for an integrated circuit solution, this lower reactance is beneficial as large inductances are more challenging (if not infeasible) to integrate.

Even though the measurements presented in this study are for a specific North American sport car, we believe that our results can easily be extended to other vehicles. This is based on the fact that the loads dominate the behavior of the access impedance, and that the battery and lamps studied here are standard for several other vehicles. It would be interesting to expand this study to other vehicle loads, like radio, ECU, air conditioning, or steering wheel controls. However, we must also note that measurement of these loads presents particular challenges, such as: a) built-in electronic protections, e.g., anti-theft radio system, b) various possible electronic states, for example, for the ECU, and c) the need for large amounts of current in the ON state (few tens of amperes) which presents a challenge for DC biased VNA measurements. Another interesting extension is a comparison of the impedance of different types of batteries such as lead-acid, NiMH, and Li-ion

#### IV. CONCLUSION

In this paper, we have presented an experimental study of access impedance in VPLC with the purpose of gaining further insights towards the understanding and emulation of the VPLC network. In particular, we present experimental measurement data for the vehicle battery, as well as for the rear, front, and trunk lights. These measurements are combined with input impedance measurements at selected plug-in nodes to calculate their combined effect in determining the total access impedance as would be seen by a PLC device connected in parallel to the same nodes. The results show how the inductive nature of the battery and lamps dominates the shape of the access impedance. This has important implications for the potential design of adaptive impedance matching circuits. As for all VPLC measurement campaigns, this study is tied to a specific car model. However, given the dominance of the battery and lamp loads on the overall results, we expect that the observations from this study can be extended and applied to other vehicles.

#### REFERENCES

- [1] M. Schwartz, "Carrier-wave telephony over power lines- early history," *IEEE Communications Magazine*, vol. 47, no. 1, pp. 14–19, January 2009.
- [2] H. C. Ferreira, L. Lampe, J. Newbury, and T. G. Swart, *Power Line Communications: Theory and Applications for Narrowband and Broadband Communications over Power Lines*, John Wiley & Sons, 2010.
- [3] S. Galli, A. Scaglione, and K. Dostert, "Broadband is Power: Internet Access through the Power Line Network," *IEEE Communications Magazine*, Feature Topic, vol. 31, no. 5, May 2003.
- [4] F. Nouvel, G. El Zein, and J. Citerne, "Code division multiple access for an automotive network over power lines," in *Proc. IEEE Vehicular Technology Conference (VTC)*, pp. 525–529, June 1994.
- [5] Y. Marayanka, "Wiring reduction by battery power line communication," *IEE Seminar on Passenger Car Electrical Architecture*, pp. 8/1–8/4, June 2000.
- [6] A. Schiffer, "Statistical channel and noise modeling of vehicular DC lines for data communications," in *Proc. IEEE Vehicular Technology Conference (VTC)*, pp. 158–162, May 2000.
- [7] P. A. Janse van Rensburg, and H. C. Ferreira, "Automotive powerline communications: favourable topology for future automotive electronic trends," *International Symposium on Power Line Communications and Its Applications (ISPLC)*, pp. 103–108, March 2003.
- [8] T. Huck, J. Schirmer, T. Hogenmüller, and K. Dostert, "Tutorial about the implementation of a vehicular high speed communication system," in *Proc. International Symposium on Power Line Communications and Its Applications (ISPLC)*, pp. 162–166, April 2005.
- [9] M.O. Carrion, M. Lienard, and P. Degauque, "Communication over vehicular DC lines: propagation channel characteristics," in *Proc. International Symposium on Power Line Communications and Its Applications (ISPLC)*, pp. 2–5, March 2006.
- [10] W. Gouret, F. Nouvel, and G. El-Zein, "Powerline communication on automotive network," in *Proc. IEEE Vehicular Technology Conference (VTC-Spring)*, pp. 2545–2549, April 2007.
- [11] M. Lienard, M.O. Carrion, V. Degardin, and P. Degauque, "Modeling and analysis of in-vehicle power line communication channels," *IEEE Transactions on Vehicular Technology*, vol. 57, no. 2, pp. 670–679, March 2008.
- [12] F. Nouvel, P. Maziero, "X-by-wire and intra-car communications: power line and/or wireless solutions," in *Proc. International Conference on Intelligent Transport Systems Telecommunications (ITST)*, pp. 443–448, October 2008.
- [13] M. Mohammadi, L. Lampe, M. Lok, S. Mirabbasi, M. Mirvakili, R. Rosales, P. van Veen, "Measurement study and transmission for in-vehicle power line communication," in *Proc. International Symposium on Power Line Communications and Its Applications (ISPLC)*, pp. 73–78, March–April 2009.
- [14] G. Leen and D. Heffernan, "Expanding automotive electronic systems," *Computer*, vol. 35, no. 1, pp. 88–93, January 2002.
- [15] N. Navet, Y. Song, F. Simonot-Lion, and C. Wilwert, "Trends in automotive communication systems," *Proceedings of the IEEE*, vol. 93, no. 6, pp. 1204–1223, June 2005.
- [16] F. Benzi, T. Facchinetti, T. Nolte, L. Almeida, "Towards the powerline alternative in automotive applications," in *Proc. IEEE International Workshop on Factory Communication Systems (WCFS)*, pp. 259–262, May 2008.
- [17] Yamar Electronics, Yamar SIG60 Powerline Transceiver, [Online] accessed on February 4, 2011, available at: <http://www.yamar.com/datasheet/DS-SIG60.pdf>
- [18] Maxim, MAX2981 Integrated Powerline Communication Analog Front-End Transceiver and Line Driver, [Online] accessed on February 4, 2011, available at: <http://www.maxim-ic.com/datasheet/index.mvp/id/6333>
- [19] W. Gouret, F. Nouvel, and G. El-Zein, "High Data Rate Network Using Automotive Powerline Communication," in *Proc. International Conference on Intelligent Transport Systems Telecommunications (ITST)*, pp. 64–67, June 2007.
- [20] P. Tanguy, F. Nouvel, and P. Maziearo, "Power Line Communication standards for in-vehicule networks," in *Proc. International Conference on Intelligent Transport Systems Telecommunications (ITST)*, pp. 533–537, October 2009.
- [21] C. Chenghui, D. Dong, G. Jingtian, L. Zhiyu, and Z. Hua, "Battery-charging model to study transient dynamics of battery at high frequency," in *Proc. IEEE Region 10 Conference on Computers, Communications, Control and Power Engineering (TENCON)*, vol. 3, pp. 1843–1846, October 2002.